Biogenesis of Processing-Competent Secretory Organelles in Vitro†

J. Michael Andresen‡ and Hsiao-Ping H. Moore*

Department of Molecular and Cell Biology, University of California, Berkeley, California 94720-3200

Received June 19, 2001; Revised Manuscript Received August 17, 2001

ABSTRACT: Propeptide processing occurs in specific compartments of the secretory pathway, but how these processing-competent organelles are generated from their processing-incompetent precursor compartments is unknown. To dissect the process biochemically, we have developed a novel cell-free system reconstituting the production of processing-competent secretory granules in AtT-20 cells. Using donor membranes containing [^{35}S]sulfate labeled pro-opiomelanocortin (POMC)[5] in the trans-Golgi, we can reconstitute cytosol- and ATP-dependent prohormone processing as well as incorporation of processed ACTH into immature secretory granules (ISGs). Under limiting cytosol conditions, both reactions are greatly stimulated by ADP-ribosylation factor 1 (ARF1) but not by the GDP-bound ARF1 T31N mutant. pH studies show that lumenal acidification, most likely due to ARF-mediated sorting of proton pumps and leaks during budding, confers processing competency to the resulting organelle. Surprisingly, comparison of onset of processing and ISG release reveals that they are distinct biochemical processes with different kinetics and separate cytosolic requirements. Moreover, ARF regulates the onset of prohormone processing but not ISG release. Our data suggest a two-step mechanism (onset of processing followed by ISG release) for the production of processing-competent organelles from the trans-Golgi and provide the first system with which these two steps may be individually dissected.

Proteolytic processing in the secretory pathway is an important and universal mechanism for the controlled production of bioactive molecules. A variety of proteins, ranging from peptide hormones, neuropeptides, growth factors, receptors, viral surface glycoproteins, matrix metalloproteases (MMPs)[1], and cell adhesion molecules, are generated from their inactive precursors by limited endoproteolysis at specific pairs of basic residues. A family of enzymes, known as subtilisin-like proprotein convertases (SPCs), catalyzes this type of processing in mammalian cells (reviewed in refs *1*−*3*). Altered processing has been implicated in several human diseases, such as multiple endocrine deficits and obesity due to SPC3 deficiency (*4*, *5*) and tumor cell invasion resulting from MMP activation by elevated expression of SPC4 (*6*).

Proprotein processing is a tightly regulated process. Individual SPCs have specific tissue distribution patterns; SPC2 (or PC2) and SPC3 (or PC1/3) are primarily expressed in neuroendocrine cells whereas SPC1 (or Furin) is more ubiquitously expressed. Within each tissue, SPC activities are carefully controlled by intracellular compartmentalization to ensure processing of only the correct substrates. However, since all SPCs are synthesized at the ER and travel through the secretory pathway to reach their sites of action, they are present in multiple compartments. Mechanisms must therefore be in place to prevent inappropriate expression of SPC activities in earlier compartments of the secretory pathway. Recently, several inhibitors that could serve this function have been found for a number of SPCs. For example, the amino-terminal prodomain of Furin, which is generated by autocatalytic cleavage in the ER, acts as an autoinhibitor to prevent cleavage of heterologous substrates (*7*). Two endogenous inhibitors, 7B2 and proSAAS, have also been identified and shown to be specific for SPC2 and SPC3, respectively (*8*−*10*). SPC1 functions in the constitutive pathway and becomes activated when it encounters the trans-Golgi network (TGN), while SPC2 and SPC3 are thought to be activated in secretory granules of the regulated secretory pathway. Apparently, upon reaching these compartments the inhibitors undergo further cleavages and dissociate from their bound SPCs to release the active enzymes.

The above scheme of compartment-specific activation of SPCs requires that the inhibitors be destroyed at the target organelles. How this is accomplished is not well understood. It is thought that the milieu of late secretory compartments provides the necessary trigger for SPC activation (*7*, *11*), but how these organelles acquire their unique processing-conducive environment remains a mystery. Recent physiological experiments have revealed important differences in the ion-transporting properties between distal and proximal compartments of the secretory pathway (*12*, *13*). Presumably, it is sorting of critical membrane transporters within the secretory path that creates processing-competent organelles

† This work was supported by grants from the National Science Foundation (MCB-9983342), University of California Cancer Research Coordinating Committee, and University of California Faculty Research Grants (to H.-P.M.). J.M.A. was supported by a Howard Hughes Medical Institute Pre-doctoral Fellowship.

* To whom correspondence should be addressed.

‡ Present address: Center for Cancer Research, Massachusetts Institute of Technology, Cambridge, MA 02139.

[1] Abbreviations: ACTH, adrenocorticotropic hormone; ARF, ADP-ribosylation factor; BafA1, bafilomycin A1; BFA, brefeldin A; GAG, glycosaminoglycan; ISG, immature secretory granule; MMP, matrix metalloprotease; NEM, *N*-ethylmaleimide; SPC, subtilisin-like proprotein convertase; POMC, pro-opiomelanocortin; PLD, phospholipase D; PtdIns, phosphatidylinositol; V-ATPase, vacuolar H^+-ATPase.

10.1021/bi0112762 CCC: $20.00
Published on Web 10/03/2001

from processing-refractory precursor compartments. As a first step toward understanding this process, we have developed a cell-free system to dissect the biogenesis of processing-competent organelles in vitro. Although there are several existing systems that reconstitute packaging of secretory products into regulated secretory granules, none is appropriate for our purpose. In the GH_3 cell system developed by Xu and Shields (*14*), the donor TGN compartment is already processing-competent and can promote SPC2-catalyzed processing of prosomatostatin. In the PC-12 cell model of Tooze et al. (*15*), the secretory marker secretogranin II does not undergo proteolytic processing.

We have chosen the AtT-20 neuroendocrine cell line as our model system. These cells store and secrete adrenocorticotropic hormone (ACTH), which is synthesized as the large prohormone precursor pro-opiomelanocortin (POMC) (*16*). Hormone processing occurs in the regulated secretory pathway and is catalyzed by the enzyme SPC3 (*17*−*19*). In vivo studies in AtT-20 cells have shown that onset of POMC processing and packaging into nascent granules both happen quickly following sulfation of POMC in the late Golgi. Immediately after a 5-min pulse labeling with radioactive sulfate, POMC was retained in a large membrane compartment that co-localized with the Golgi apparatus by sucrose gradient centrifugation. If the pulse label was followed by a 15-min chase, two events occurred: (1) SPC3 started processing POMC into intermediate peptides and mature ACTH, and (2) the labeled proteins moved to a small vesicular membrane compartment corresponding to newly formed immature secretory granules (ISGs) (*20*). This cell line therefore provides an ideal system to study the formation of processing-competent secretory granules from their precursor trans-Golgi compartment.

We have developed a cell-free system using AtT-20 cells and demonstrated that the formation of ISGs from the trans-Golgi requires at least two independently regulated steps. Starting with partially purified Golgi stacks from pulse-labeled cells, our system reconstitutes formation of processing-competent organelles in vitro during an incubation with ATP and cytosol. Using separate assays to monitor the onset of POMC processing and ISG release, we discover that these represent biochemically distinct events. We demonstrate that the small GTPase ARF is required for the earlier step of onset of prohormone processing but that it is not required for the final step of ISG release. We provide a model that relates our biochemical results to the morphological data of progranule formation in the fenestrating trans-Golgi cisternae as described by Rambourg et al. (*21*), and suggest a role for ARF in ISG formation that is well before the actual release of ISGs.

MATERIALS AND METHODS

Solutions and Reagents. Sulfate starvation buffer is 110 mM NaCl, 5.4 mM KCl, 0.9 mM Na_2HPO_4, 10 mM $MgCl_2$, 1 mM $CaCl_2$, 1 g/L glucose, and 20 mM *N*-2-hydroxyethylpiperazine-*N*′-2-ethane sulfonic acid (HEPES), pH 7.3. Buffered equimolar ethyleneglycol-bis(β-aminoethyl ether)-*N*,*N*′-tetraacetic acid (EGTA) and calcium was prepared as described (*22*). Homogenization buffer is 250 mM sucrose, 15 mM KCl, 1 mM $MgCl_2$, 2 mM EGTA, 1.29 mM equimolar EGTA/calcium, and 10 mM HEPES-KOH, pH 7.3. Standard assay buffer is the same as homogenization buffer, but with 150 mM sucrose. Crude assay buffer is 250 mM sucrose, 125 mM potassium acetate, 15 mM KCl, 5 mM NaCl, 5 mM $MgSO_4$, 4 mM magnesium acetate, 2 mM EGTA, 1.29 mM equimolar EGTA/calcium, and 10 mM HEPES-KOH, pH 7.3. The buffered free calcium concentration in all assay buffers is 100 nM. Centrifugation buffer is 1.6 mM Na_2SO_4, 1 mM magnesium acetate, 1 mM ethylenediaminetetraacetic acid (EDTA), and 10 mM HEPES−KOH, pH 7.3. ATP Regeneration System is 40 IU/mL creatine kinase (Boehringer-Mannheim, Indinapolis, IN), 2 mM creatine phosphate, 2.5 mM ATP (sodium salt, neutralized with KOH), 5 mM $MgCl_2$, and 1 mM GTP (lithium salt, neutralized with KOH). ATP Degeneration System is 75 IU/mL hexokinase (Sigma, St. Louis, MO) and 2 mM glucose. Sodium dodecyl sulfate−polyacrylamide gel electrophoresis (SDS−PAGE) buffer is 20% glycerol, 2% SDS, 10% β-mercaptoethanol, 0.008% bromphenol blue, and 125 mM tris(hydroxymethyl)aminomethane, pH 6.8. MC63 and Dyn2 antibodies were kindly provided by Dr. M. A. McNiven (*23*). Rab GDP dissociation inhibitor (GDI) was kindly provided by Dr. S. R. Pfeffer (*24*).

Cell Culture. All cells were maintained in Dulbecco's modified Eagle's medium (4.5 g/L glucose) supplemented with 10% FCS at 37 °C. AtT-20 cells were grown under 15% CO_2 at 37 °C. HeLa cells were grown under 5% CO_2 at 37 °C.

Preparation of Donor Membranes. Up to three semi-confluent 15 cm dishes of AtT-20 cells were prepared at one time for radiolabeling experiments. Cells were rinsed and then incubated for 30 min at 37 °C in sulfate starvation buffer. Cells were then rinsed in starvation buffer and labeled in 2.5 mL starvation buffer with 2 mCi/ml $Na_2{}^{35}SO_4$ (1325 Ci/mmol, NEN Life Sciences, Boston, MA) for 3.5 min in a 37 °C water bath. They were then immediately placed on ice (Figures 1A and 2−6) or chased at 37 °C for 10 min before being placed on ice (Figure 1B). Cells were rinsed twice in ice-cold homogenization buffer, scraped with a rubber policeman, and brought to a final volume of 1 mL with homogenization buffer. The cell suspension was passed three times through a 23 gauge needle and homogenized with 16 passes through an EMBL ball homogenizer. The homogenate was centrifuged at 1300*g* for 5 min to bring down nuclei. The resulting postnuclear supernatant was used directly in the crude assays (Figure 1). For the refined assays (Figures 2−6), the postnuclear supernatant was centrifuged at 16000*g* for 5 min to separate the Golgi and other large membranes from the cytosol. The membrane pellet was resuspended by repeatedly pipetting in 350 μL Homogenization Buffer. The protein concentration of the resuspended membranes was determined. The membranes were washed in 1 mL standard assay buffer and centrifuged at 16,000*g* for 5 min. The membrane pellet was resuspended to a concentration of 10 mg/mL in Homogenization Buffer based on the initial concentration determination, even though typically 30% of the total protein was lost in the wash. This was a time-saving maneuver to reduce processing time. This membrane suspension was used as the donor membrane fraction in the in vitro assay. Typically, this procedure resulted in 100 μL of donor membranes per 15 cm dish harvested. Varying the donor membrane concentration between 5 mg/mL and 15 mg/mL had no effect on the processing assay (data not shown).

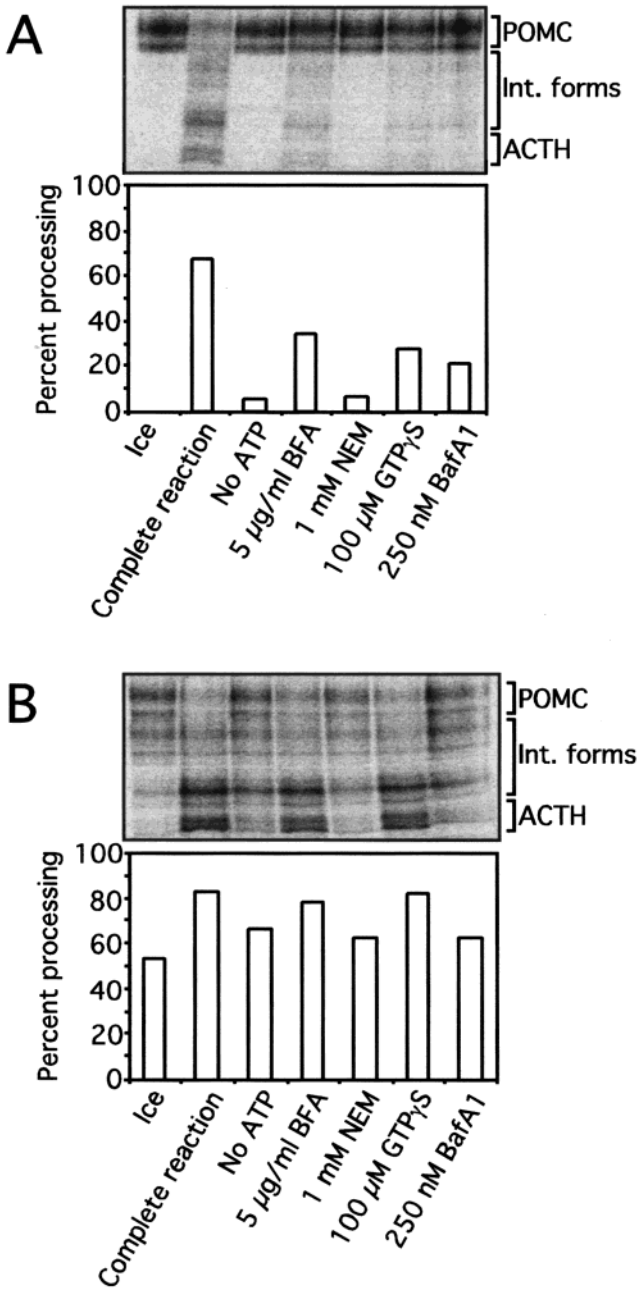

FIGURE 1: POMC processing can be reconstituted in an AtT-20 postnuclear supernatant. In vitro reactions were set up using post-nuclear supernatants prepared from cells that had been pulse-labeled with [^{35}S]sulfate for 3.5 min and either harvested immediately or after a 10 min chase. The ice reactions were kept on ice while the rest were incubated at 37 °C for 90 min. The complete reactions had no additions other than an ATP regeneration system. The remaining reactions were set up as in the complete reaction but with added inhibitor: an ATP depletion system instead of a regeneration system, 5 μg/mL BFA, 1 mM NEM added on ice for 15 min followed by 2 mM DTT for 15 min, 100 μM GTPγS, or 250 nM BafA1. (A) Post-nuclear supernatant made after a pulse label of POMC in the trans-Golgi. (B) Post-nuclear supernatant made after a pulse label and a 10-min chase to allow migration of labeled POMC to ISGs.

Preparation of Cytosol and ARF. Cytosol was prepared with unstarved, unlabeled AtT-20 or HeLa cells grown in 15 cm dishes. Typically, 24 dishes were prepared at one time. Cells were placed on ice and washed in standard assay buffer. Cells were scraped and homogenized as above, but in standard assay buffer. Homogenate was centrifuged at 200000*g* for 1 h to remove cellular membranes. The supernatant cytosol (typically 6 to 8 mg/mL) was aliquoted, flash frozen in liquid nitrogen, and stored at −80 °C. Recombinant myristoylated ARF1 was prepared as described (*25*). Bacterial expression strains for wild-type ARF1, ARF1 Q71L, and ARF1 T31N that coexpressed yeast N-myristoyltransferase were kindly provided by Dr. D. Shields (*26*).

In Vitro Reaction. The crude in vitro reaction (Figure 1) consisted of 180 μL of postnuclear supernatant and 20 μL of a mixture containing 400 IU/mL creatine kinase, 20 mM creatine phosphate and 2.5 mM ATP in crude assay buffer. The refined in vitro reactions (Figures 2−6) consisted of the indicated components along with 5 μL donor membranes, ATP Regeneration System, and standard assay buffer in a total volume of 30 μL. Reactions were set up on ice and then incubated in a 37 °C water bath for 60 min unless otherwise indicated. After the in vitro reaction, the samples were processed for the POMC processing assay, the granule release assay, or the constitutive vesicle release assay as described below.

POMC Processing Assay. Following incubation at 37 °C, in vitro reactions were centrifuged at 100000*g* for 20 min. Pellets were resuspended in SDS−PAGE buffer, run on 15% SDS−PAGE, and exposed to a PhosphorImager cassette for 1−2 days (Molecular Dynamics, Sunnyvale, CA). Gels were quantified using Molecular Dynamics PhosphorImager software. The amount of processed POMC existing in a control reaction kept on ice was subtracted from all other processed POMC amounts quantified from other lanes to eliminate background sulfated proteins. Processing efficiency was calculated as the amount of processed POMC (minus the background from the reactions kept on ice) divided by the total amount of processed and unprocessed POMC: percent processing = (I + A)/(P + I + A) where "P" is POMC, "I" is intermediate forms, and "A" is ACTH.

Granule release assay. Following incubation at 37 °C, in vitro reactions were placed on a 0.5 mL pad of 360 mM sucrose and 300 mM KCl in centrifugation buffer and centrifuged at 16000*g* for 5 min. Large membranes such as the Golgi moved through this pad (P1), while small vesicular membranes containing newly formed granules were retained in the supernatant (S1). The supernatant was removed and diluted in 0.5 mL of H_2O. The mixture was centrifuged at 150000*g* for 60 min after addition of 20 μg of unlabeled donor membranes as carrier. This vesicle pellet (P2) and the Golgi pellet (P1) were processed for SDS−PAGE as above. Granule release efficiency was calculated as amount of radioactivity in the vesicle pellet (P2) divided by the total amount of radioactivity in both Golgi and vesicle pellets (P1 + P2): percent release = V/(G + V) where "G" is the Golgi pellet (P1) and "V" is the vesicle pellet (P2).

Constitutive Vesicle Release Assay. For glycosaminoglycan (GAG) chain experiments, the cells were labeled and donor membranes prepared as above, except that 0.5 mM 4-methylumbelliferyl β-D-xyloside was added to the starvation buffer and labeling was carried out with 200 μCi/mL $Na_2{}^{35}SO_4$ in the presence of β-D-xyloside. Following the in vitro assay, the Golgi and vesicle fractions were separated as in the granule release assay. Pellets were resuspended in 500 μL of 0.2% Triton X-100, and sulfate-labeled GAG chains were quantified by the cetylpyridinium chloride assay (*27*). Vesicle release efficiency was calculated as the percentage of GAG

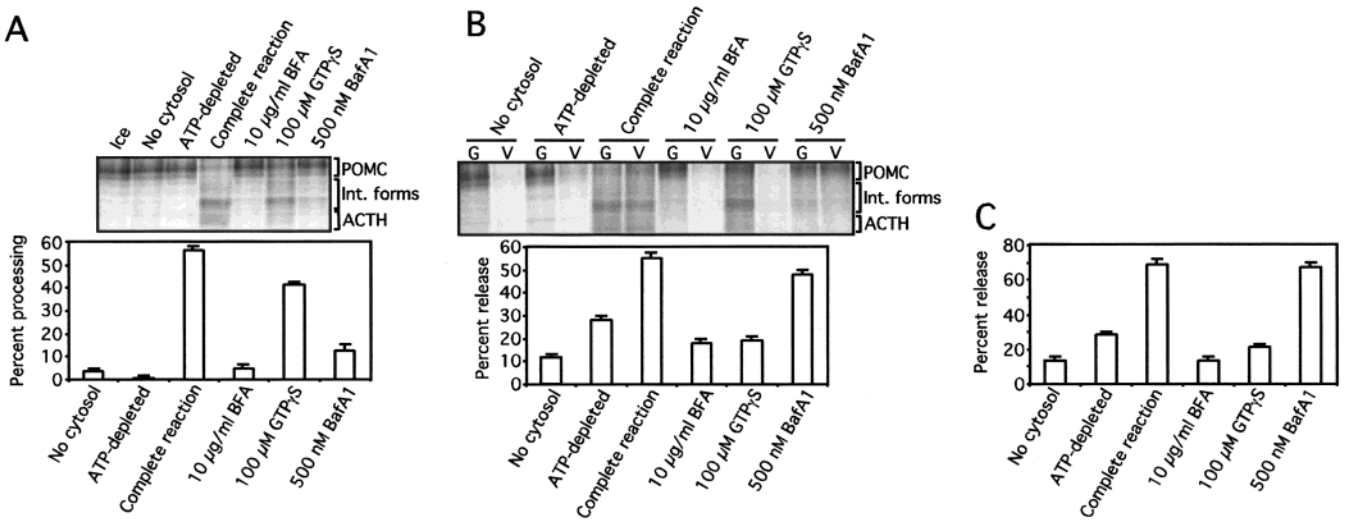

FIGURE 2: POMC processing and ISG release can be reconstituted with purified membranes and exogenous cytosol. In vitro reactions were set up using partially purified AtT-20 Golgi membranes from cells that had been pulse labeled with [^{35}S]sulfate and harvested without a chase. The complete reaction was set up with 2 mg/mL of exogenous AtT-20 cytosol and an ATP regeneration system. The remaining reactions were set up with a single change: no exogenous cytosol, an ATP depletion system instead of an ATP regeneration system, 10 μg/mL BFA, 100 μM GTPγS, or 500 nM BafA1. Note that in contrast to the crude assay in Figure 1, these refined assays contained 1 mM GTP as a part of the standard assay mixture. Representative results from SDS−PAGE analysis are shown. Quantitative data points represent the average of six identical reactions. Error bars represent the standard errors of the means. (A) POMC processing assay. The extent of POMC processing at the end of the reaction was analyzed by SDS−PAGE. The ice reaction was kept on ice while the rest were incubated at 37 °C for 60 min. Quantitation was done by measuring the percentage of all POMC-derived peptides that were converted to intermediate forms or mature ACTH. The ice control was set to zero. (B) Granule release assay. After incubations, Golgi membranes (G) were separated from released vesicles (V) by differential centrifugation. Quantitation was done by measuring the percentage of all POMC-derived peptides present in the vesicle pellet. (C) Constitutive vesicle release assay. In vitro reactions were set up with AtT-20 Golgi membranes as above, except that the cells were pulse-labeled in the presence of a membrane-permeant xyloside to induce synthesis of free GAG chains as a constitutive marker. After incubations, Golgi membranes (G) were separated from released vesicles (V) by differential centrifugation. Quantitation was done by measuring the percentage of free GAG chains in the vesicle pellet.

chains in the vesicle pellet: percent release = V/(G + V) where "G" is the Golgi pellet (P1) and "V" is the vesicle pellet (P2).

Nomenclature. The "POMC processing assay" (Figure 2A) reconstitutes both the onset of processing (which is sensitive to ARF antagonists) and the slow proteolytic processing event itself (which is sensitive to inhibitors of the H^+ V-ATPase). The "granule release assay" (Figure 2B) reconstitutes both the onset of processing (which is sensitive to ARF antagonists) and the granule release step (which is not sensitive to ARF antagonists, but is sensitive to low concentrations of GTPγS). Specific observations about the individual processes of "onset of processing" and "granule release" can only be made by comparing results from the POMC processing assay and the granule release assay.

RESULTS

Characterization of POMC Processing in Vitro. We first used a crude postnuclear supernatant prepared from [^{35}S]sulfate pulse-labeled AtT-20 cells to reconstitute POMC processing in vitro. When an ATP regeneration system was added to the crude cell homogenate and the reaction was incubated at 37 °C, >65% of labeled POMC was processed into intermediate forms and ACTH while a control reaction kept on ice showed little processing (Figure 1A, compare complete reaction to ice control). Processing required ATP, since in the presence of an ATP depleting system only <5% of POMC was processed. Importantly, the observed processing was significantly inhibited by the fungal metabolite brefeldin A (BFA), or the nonhydrolyzable GTP analogue guanosine 5′[γ-thio]triphosphate (GTPγS). Both of these reagents block vesicle budding; BFA interferes with GTP exchange by certain guanine nucleotide exchange factors for ARF (*28*, *29*), while GTPγS alters the activity of a variety of GTPases. These data indicate that processing requires exit of POMC from the sulfation compartment. It follows that the donor sulfation compartment is processing-incompetent. Presumably, during an incubation with ATP at 37 °C processing-competent organelles are generated from the sulfation compartment by vesicle budding. Supporting this idea, differential centrifugation experiments from the same reactions showed that free vesicles were released in the complete reaction, but not when inhibited by ATP depletion or with GTPγS (data not shown; see also Figure 2B).

The in vitro processing reaction was also inhibited by *N*-ethylmaleimide (NEM) or bafilomycin A1 (BafA1), each of which inhibits the H^+ V-ATPase (*30*, *31*) (Figure 1A). Since SPC3 has an acidic pH optimum (*32*−*34*), these results are consistent with the notion that the acidic environment generated by the V-ATPase is necessary for POMC processing.

The same in vitro reaction can be set up using cells that have been pulse labeled and chased for 10 min in vivo before being homogenized (Figure 1B). The chase period corresponds to the time required for most of the labeled POMC products to move from the Golgi into budded granules (*20*). Although some processing of POMC had already started by the end of this 10-min chase, completion of the processing reaction with further cleavage of POMC into ACTH could still be reconstituted in vitro (Figure 1B, compare complete

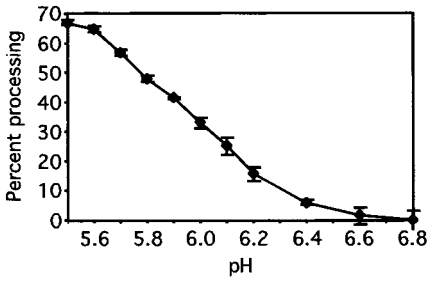

FIGURE 3: Acidic conditions are sufficient to trigger processing of POMC by SPC3. Pulse-labeled AtT-20 donor membranes were made as in Figure 2A. Membranes were incubated without cytosol or ATP for 60 min at 37 °C in buffers of indicated pHs. The percentage of POMC processing was then quantified and plotted as a function of the incubation pH.

reaction to control reaction kept on ice). This reaction now exhibited a different inhibitor profile, however. In contrast to cells harvested immediately after the pulse labeling, addition of BFA or GTPγS after the 10-min chase no longer inhibited further processing of POMC. Thus, these reagents do not directly compromise SPC3 activity. Because BFA and GTPγS block processing when added immediately after a pulse label (Figure 1A) but do not block further processing following a 10-min chase (Figure 1B), we can conclude that they block movement of POMC to the site of processing but not POMC processing itself.

In contrast to BFA and GTPγS, reagents that affect activity of the V-ATPase such as ATP depletion, NEM, or BafA1 did block further processing of POMC even when added after a 10-min chase (Figure 1B). Most likely, processing-competent organelles already formed in vivo before preparation of the cell homogenate. Thus, the only requirement for processing during the in vitro incubation is to allow acidification of the granule lumen by the ATP-driven H^+ pump.

Formation of Processing-Competent Granules from Donor Golgi *Membranes.* Our ultimate goal is to define the cytosolic requirements for formation of processing-competent organelles. We therefore refined the above crude assay by separating pulse-labeled Golgi membranes from cytosolic components by centrifugation. When the isolated membrane fraction was added to exogenous cytosol and an ATP regeneration system, POMC processing could be reconstituted to a similar extent as in total cell homogenate (Figure 2A). This refined assay was completely dependent on added cytosol; no processing occurred in Golgi membranes incubated at 37 °C without cytosol even though ATP was present to drive the V-ATPase (Figure 2A, compare complete reaction to reaction with no cytosol). As in the crude in vitro reaction, processing was inhibited by ATP depletion, BFA or BafA1 (Figure 2A, compare the complete reaction to reactions with added BFA, BafA1, or ATP depletion system). The only difference we noted is that 100 μM GTPγS, which reduced processing to <40% of control in the crude assay, produced a much smaller effect ($\sim$70% of control) in the refined assay (see Figure 4A for the full titration curve). This discrepancy is most likely due to extra (1 mM) GTP added to the refined assay. Cytosol was not needed when reactions were set up with Golgi membranes prepared from cells that had been chased for 10 min before harvesting − under conditions similar to Figure 1B (data not shown). Together, these results demonstrate that cytosolic factors are required

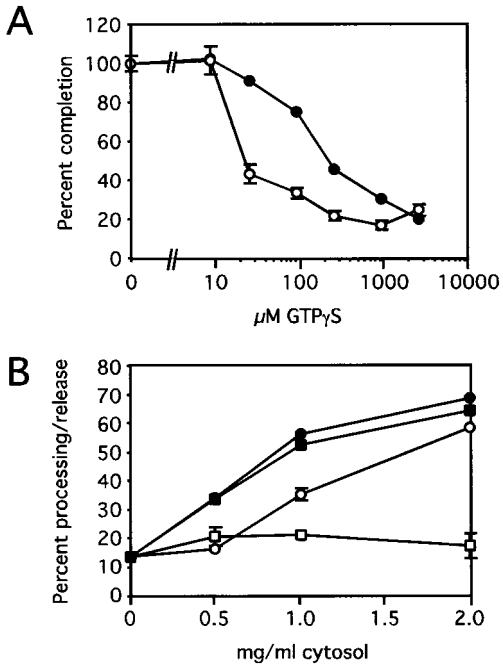

FIGURE 4: Granule formation in vitro requires two steps that are regulated independently. (A) GTPγS inhibits the granule release assay with greater potency than the POMC processing assay. In vitro reactions were set up as in Figure 2A with 2 mg/mL AtT-20 cytosol and an ATP regeneration system in the presence of increasing concentrations of GTPγS. Reactions were then assayed for POMC processing (filled circles) or granule release (open circles). The only difference between the data points for a given GTPγS concentration is the way in which the in vitro reaction was processed. The reactions themselves were identical for a given concentration. Note that all reactions were done under standard assay conditions, which included 1 mM GTP. Reactions were all performed in quadruplicate. Error bars represent the standard errors of the means and were omitted for the data points representing POMC processing reactions, as the standard errors were all under 1.5%. (B) HeLa cytosol supports the POMC processing assay but not the granule release assay. Granule formation reactions were set up with varying concentrations of AtT-20 cytosol (circles) or HeLa cytosol (squares). Reactions were then quantified for POMC processing (closed symbols) or granule release (open symbols). Granule release reactions were performed in duplicate. Error bars represent the standard errors of the means.

for the movement of POMC from the site of sulfation to the initial site of processing.

We next employed a differential centrifugation assay to test if POMC processing is correlated with its packaging into newly formed secretory granules. In vitro reactions were carried out as above and the resulting mixture was centrifuged through a sucrose pad at intermediate speed (16000*g* for 5 min) to bring down large donor Golgi membranes (indicated by "**G**"). The supernatant was then subject to high-speed centrifugation (150000*g* for 60 min) to recover small vesicular membranes including ISGs (indicated by "**V**"). Like the POMC processing assay, this granule release assay was dependent on cytosol and ATP and was effectively inhibited by BFA or 100 μM GTPγS (Figure 2B). In complete reaction supplemented with ATP and cytosol, a significant amount of labeled POMC products was found in the vesicular fraction presumably in budded ISGs. Under no cytosol, ATP-depleted, BFA, or GTPγS treated conditions, radiolabeled materials did not enter the vesicular fraction and instead were recovered only in the donor Golgi membranes. This cell-free system thus recapitulates in vitro both onset of POMC

processing and release of granules from the Golgi, in a manner similar to what was documented in vivo (*20*).

Interestingly, while BafA1 inhibited processing of POMC to <20% of control (Figure 2A), ISGs were released with >80% efficiency in the presence of the V-ATPase inhibitor (Figure 2B). Dissipation of the proton gradient across the Golgi membrane thus does not appear to interfere with granule formation.

We also examined formation of constitutive vesicles in our system by inducing GAG chain synthesis in the Golgi of AtT-20 cells (*35*). GAG chains travel in bulk flow through the secretory pathway and are secreted constitutively (*27*). Like POMC, GAG chains can be labeled in the late Golgi of AtT-20 cells with radioactive sulfate (*36*). We examined the in vitro formation of constitutive vesicles containing sulfated GAG chains using a separate vesicle release assay that measures release of GAG chains instead of POMC-derived peptides. No qualitative differences were detected between release of POMC-derived peptides and GAG chains (Figure 2C). Both were inhibited by addition of BFA, GTPγS, or an ATP depletion system; both were unaffected by BafA1. In vitro release of ISGs and constitutive vesicles in PC12 cells also show few significant qualitative differences (*15*).

Lumenal Acidification: The Key Factor Conferring Processing Competency to Granules. The above experiments indicate that processing-competent organelles can form from the trans-Golgi by vesicle budding. Since acidification by the V-ATPase is necessary for POMC processing (Figures 1 and 2), we tested if it is also sufficient to trigger processing. Isolated AtT-20 Golgi membranes were incubated at 37 °C in the absence of ATP and cytosol; under this condition, granules were not formed and POMC was trapped in the donor compartment as the unprocessed precursor (Figure 2, panels A and B). We reason if acidification as a result of vesicle budding is what confers processing competency to new granules, then we should be able to bypass the requirement for budding by lowering the pH of the donor organelle. Since Golgi membranes are leaky to protons (*12*, *13*, *37*), we can lower the Golgi lumenal pH by simply lowering the pH of the incubation buffer. As shown in Figure 3, processing of POMC indeed occurred under nonbudding conditions (no ATP, no cytosol) as long as the pH of the incubation buffer was lowered to below 6.2. The more acidic the buffer, the greater the extent of POMC processing. We conclude that a low-pH environment is not only necessary but also completely sufficient to allow POMC processing in vitro.

Relationship between Onset of POMC Processing and Granule Release. The above data show that onset of POMC processing occurs concomitantly with release of new granules. This is consistent with earlier immunocytochemical data suggesting that POMC is packaged into granules before its proteolytic cleavage (*38*, *39*). However, a careful examination of our in vitro reactions indicates that POMC processing and release of ISGs are likely to be distinct biochemical events. This was first evident when we examined the granule release assay (Figure 2B, lanes labeled "complete reaction"), where a significant fraction of the processed POMC peptides was recovered in the Golgi (G) instead of the vesicle (V) fraction. The effect was even more noticeable in reactions carried out with 100 μM GTPγS (Figure 2B, lanes labeled "100 μM GTPγS"); at this concentration of GTPγS, some POMC processing still took place but none of the processed peptides was found in the vesicle fraction. These data indicate that POMC processing could occur in the absence of granule release, suggesting that acquisition of processing competency and release of new granules may in fact be two separate events.

To examine this more closely, we compared the dose response curves for GTPγS of the POMC processing assay and the granule release assay (Figure 4A). Onset of processing was inhibited only at relatively high concentrations of GTPγS; 50% inhibition was observed at 180 μM. Release of granules from the Golgi, on the other hand, was inhibited at much lower GTPγS concentrations; 50% inhibition was observed at 20 μM GTPγS. These titration curves thus explain why 100 μM GTPγS potently inhibited ISG release while exerting only a moderate effect on POMC processing (Figure 2). These data suggest that onset of processing is regulated by a low-affinity GTPase whereas granule release is regulated by a high-affinity GTPase.

Note that we have used the term "*onset* of processing" to indicate the step in which the processing apparatus becomes activated. This is to be distinguished from "processing" itself, which is a slow process that continues long after the initial activation step.

Further evidence for separate regulation of the onset of processing and granule release comes from examining cytosol prepared from different sources (Figure 4B). Cytosol from AtT-20 cells supported both POMC processing and granule release assays. Surprisingly, cytosol prepared from HeLa cells (lacking a regulated secretory pathway) also supported the POMC processing assay and did so at the same concentration as AtT-20 cytosol. In contrast, HeLa cytosol was completely inactive in the granule release assay. This was not due to an inhibitory activity as added HeLa cytosol had no effect on reactions set up with AtT-20 cytosol (data not shown). These data suggest that certain cytosolic factors necessary only for release of ISGs are either absent from HeLa cytosol or are present in much lower concentrations than in AtT-20 cytosol. These data also demonstrate that although prohormone processing usually occurs in cells with a regulated secretory pathway, all the cytosolic factors required for onset of processing are found in cells with only a constitutive seccretory pathway. This suggests that the membrane trafficking mechanism required for onset of prohormone processing is in place in many cell types; specialized secretory cells only need to express the requisite SPCs to activate their processing capabilities.

Role of ARF in Onset of POMC Processing but Not in Granule Release. The fact that BFA blocks the in vitro reactions (Figures 1 and 2) suggests that an ARF-like protein may be involved. To examine whether ARF1 is the GTPase involved and whether it represents the GTPase regulating POMC processing or granule release, we tested the effects of purified myristoylated ARF1 in our assays. Addition of recombinant myristoylated ARF1 greatly stimulated the POMC processing assay (Figure 5A). This was most dramatically demonstrated under conditions of limiting cytosol concentrations. At 1 mg/mL of cytosol, very little processing occurred above background without added ARF. Supplementation with 20 or 80 μg/mL ARF, however, greatly stimulated processing.

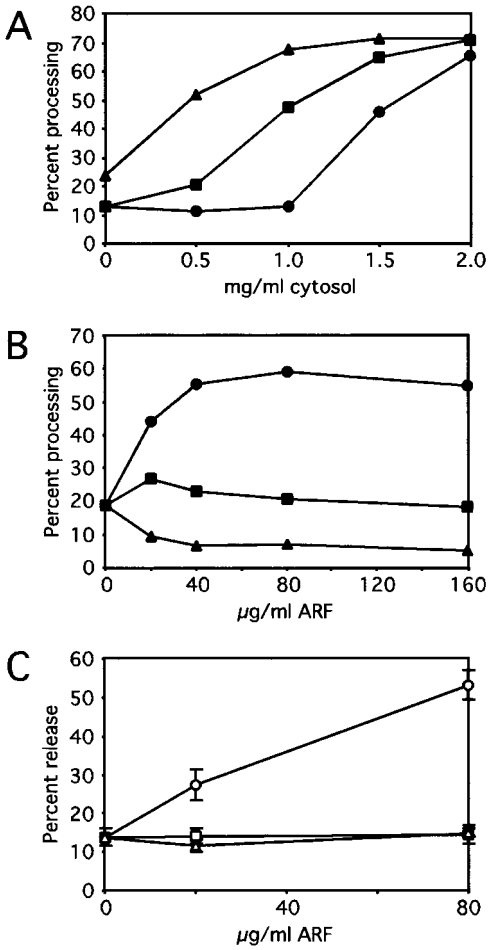

FIGURE 5: ARF stimulates both the POMC processing assay and the granule release assay. (A) In vitro reactions were set up with varying concentrations of AtT-20 cytosol in the absence of ARF (circles) or with recombinant myristoylated ARF1 added to a final concentration of 20 μg/mL (squares) or 80 μg/mL (triangles). The extent of POMC processing was quantified by the processing assay. (B, C) In vitro reactions were set up with 1 mg/mL AtT-20 cytosol and varying concentrations of wild type ARF1 (circles), constitutively GTP-bound ARF1 Q71L (squares), or constitutively GDP-bound ARF1 T31N (triangles). Reactions were then quantified for POMC processing (B, closed symbols) or granule release (C, open symbols). All reactions were performed in triplicate. Error bars represent the standard errors of the means and were omitted for data points representing POMC processing reactions, as the standard errors were all under 1.5%.

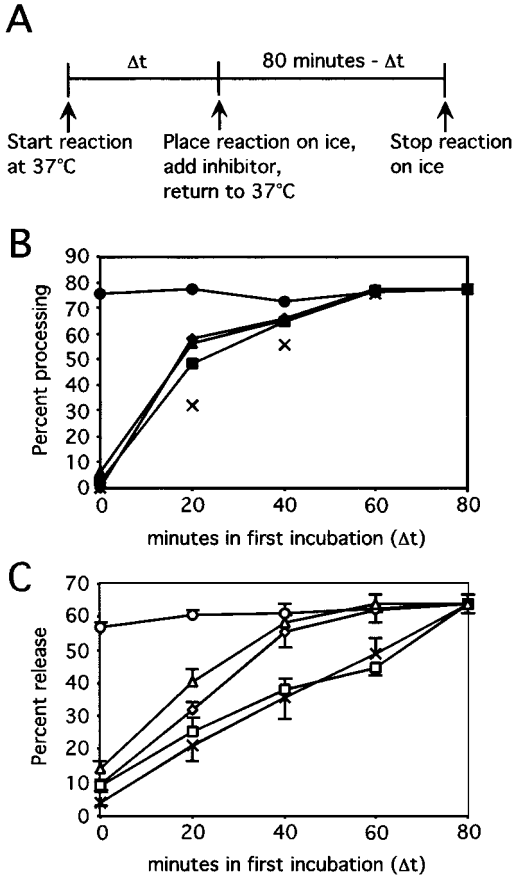

FIGURE 6: Kinetic study of inhibition reveals two regulatory steps for in vitro granule formation. In vitro reactions were set up in 2 mg/mL of AtT-20 cytosol and an ATP regeneration system. At each time point, reaction tubes were removed from 37 °C and placed on ice. Either 1 μL of an inhibitor stock or 1 μL standard assay buffer (as a positive control) was added to each appropriate tube. Reaction tubes were then replaced at 37 °C for the remainder of the 80-min incubation with the exception of the ice control tubes (crosses), which were left on ice (as a negative control). Final concentrations of inhibitors: 1 mM GTPγS (squares), 0.2 mg/mL ARF1 T31N (triangles), 10 μg/mL BFA (diamonds), or assay buffer with no inhibitor (circles). (A) Schematic diagram of the experimental design. (B) POMC processing assay. (C) Granule release assay. Granule release assay reactions were run in triplicate. Error bars represent the standard errors of the means.

Mutant forms of ARF1, on the other hand, did not stimulate processing (Figure 5B). ARF1 T31N, which is constitutively in the GDP-bound form, potently inhibited even the low level of processing provided by an assay with set up with 1 mg/mL of cytosol. ARF1 Q71L, which is constitutively in the GTP-bound form, provided some stimulation at low levels but did not stimulate to the same extent as wild-type ARF1.

The granule release assay was also stimulated by ARF1 but not by either form of mutant ARF1 (Figure 5C). Because ARF1 stimulates assays for both POMC processing (which monitors only the first step of the reaction) and granule release (which monitors both steps), ARF is most likely involved in the first step, onset of POMC processing. To further test this conclusion, we compared the kinetics of various inhibitors (Figure 6A). Granule release and POMC processing reactions were run for various amounts of time at 37 °C. At each time point, the reactions were removed from the 37 °C water bath and put on ice. One set was left on ice to indicate how far the reaction had progressed at that point. The other reactions were placed back at 37 °C for the remainder of the 80-min incubation after addition of either an inhibitor (BFA, GTPγS, or ARF T31N) or an equivalent volume of assay buffer.

For the processing reaction, the inhibitors GTPγS, BFA, or ARF T31N all inhibited progression of the reaction with the same time course ($t_{1/2} \approx 14$ min), indicating that they all act at the same stage in this process (Figure 6B). For the onset of processing, then, the latest GTPγS effect is at the same stage as the ARF antagonists (BFA and ARF T31N). This is consistent with ARF being the GTPγS-sensitive factor that regulates onset of POMC processing. Note that the inhibitors block onset of processing but do not block further processing after processing has already started. Therefore, some additional amount of processing occurred after the inhibitor was added when compared to the reaction kept on

ice (Figure 6B). This is because SPC3 is inactive on ice, while the inhibitor reactions were returned to the water bath for a second incubation during which further processing could occur. We plot the points of the ice curve with no connecting line in order to emphasize the differing kinetics between the rate of processing itself (measured in the ice control) and the rate of acquisition of processing competency (measured with addition of GTPγS, BFA, and ARF T31N). The key point of this experiment is that GTPγS inhibits onset of processing with similar kinetics as BFA and ARF T31N, indicating that they all inhibit at the same stage in this process.

This is not the case in the granule release assay (Figure 6C). Here, the GTPγS effect is well after that of the ARF antagonists BFA or ARF T31N. Addition of GTPγS inhibited this reaction at a very late stage ($t_{1/2} \approx 30$ min): no further granule release was observed at any time point beyond what had already occurred as indicated by the ice control. (The ice control is a useful control in this case, as it is not complicated by the kinetic delay of the processing reaction.) By contrast, the ARF antagonists, BFA or ARF T31N, inhibited the granule release assay with an early time course ($t_{1/2} \approx 16$ min) as in the POMC processing assay. Thus, when added at intermediate time points, these reagents allowed significantly more granule release than GTPγS (Figure 6C, compare the GTPγS curve with the BFA and ARF T31N curves). Since granule release is inhibited by GTPγS at a later stage than the ARF antagonists, a GTP-binding protein other than ARF functions to regulate granule release.

These data are all consistent with a two-step model of granule formation. In the first step, ARF works to promote onset of processing (which proceeds with a half time of 15 min based on the curve with GTPγS in Figure 6B), during which the V-ATPase provides a sufficiently acidic compartment to allow activation of SPC3. Further incubation at 37 °C allows these ISGs to be released (which proceeds with a half time of 30 min based on the curve with GTPγS in Figure 6C) so that they appear as free vesicles during differential centrifugation. This second step is regulated by a high-affinity GTP-binding protein. ARF regulates onset of POMC processing but not granule release.

DISCUSSION

A Two-Step Mechanism for the Production of Processing-Competent Granules from the trans-Golgi. We have developed a novel cell-free system that reconstitutes onset of prohormone processing and release of ISGs from partially purified Golgi stacks. Several systems have previously reconstituted proprotein processing in vitro (e.g., *14*, *40*). However, these reactions typically require only the addition of ATP or ATP regenerating systems and are not inhibited by BFA. Thus, they only reconstitute processing in a preformed compartment. In our reaction, a processing-competent organelle is produced from a donor processing-refractory compartment. We demonstrated that formation of these organelles in AtT-20 cells follows a two-step process. This conclusion is based on three lines of evidence. First, onset of processing and ISG release is inhibited by different concentrations of GTPγS (Figure 4A). Second, HeLa cytosol supports POMC processing without allowing granule release, while AtT-20 cytosol supports both processes equally well (Figure 4B). Third, GTPγS inhibits the POMC processing assay at the same step kinetically as the ARF antagonists BFA and ARF T31N, while GTPγS inhibits the granule release assay at a later stage than these ARF antagonists (Figure 6).

At intermediate concentrations of GTPγS (Figure 4A) or when reactions were set up with HeLa cytosol instead of AtT-20 cytosol (Figure 4B), POMC processing took place while granule release was completely inhibited. Onset of processing and ISG release are thus completely separable. Importantly, because processing can happen in the absence of release, we can further conclude that the onset of POMC processing must precede granule release during the reaction.

This two-step mechanism, acquisition of processing competency followed by granule release may help to explain some of the controversies in the literature. Several studies have indicated that the majority of POMC processing occurs in secretory granules (*20*, *38*, *39*). However, using a sensitive HRP-detection method, Schnabel et al. detected processed forms of POMC in the dilated rim of the Golgi complex (*41*). In light of our data, the most likely explanation is that granules gain competency for processing at an early stage during their formation from the trans-Golgi. However, since processing is a relatively slow process compared to granule release, the majority of processing probably does take place in released granules. POMC processing can be detected in the Golgi only if using highly sensitive method or if the granule release process could be slowed, as we have done using our in vitro system.

That ARF is involved in the overall process of ISG formation from the Golgi has been demonstrated in two other reconstituted systems: in both the PC12 cell in vitro assay (*42*) and the GH_3 permeabilized cell assay (*26*), release of ISGs from the TGN is regulated by ARF. There are important differences in our results, however. In the GH_3 assay, the GTP-bound ARF1 Q71L maximally stimulated granule production, consistent with its proposed function as an upstream activator of phospholipase D (PLD) (*43*). In our system, ARF1 Q71L produced a much smaller effect than wild-type ARF1 in the POMC processing assay (Figure 5B) and was completely inactive in the granule release assay (Figure 5C). These results suggest that efficient formation of processing-competent granules requires cycles of GTP hydrolysis by ARF1, an observation that is more easily explained if ARF-GTP functions to transiently recruit a cytoplasmic coat protein (*53*, *54*). The reason for this discrepancy is unclear, but it may be due to differences in the experimental system. The GH_3 assay utilizes donor compartment containing secretory products blocked at 20 °C, whereas our assay starts with products radiolabeled with sulfate. Although both are presumed to be the same TGN compartment, they may represent distinct domains of this complex organelle. The previous assays also only measure release of ISGs from the TGN, while our assays detect both granule release and onset POMC processing (Figure 2A). (Please refer to Nomenclature in Materials and Methods for a full explanation of these two assays.) This allows us to examine the process of ISG formation with higher resolution than was previously possible. By comparing the POMC processing assay and the granule release assay, we show that ARF is not involved in the ISG release step. Rather, ARF acts at the earlier step of onset of prohormone processing (Figure 6).

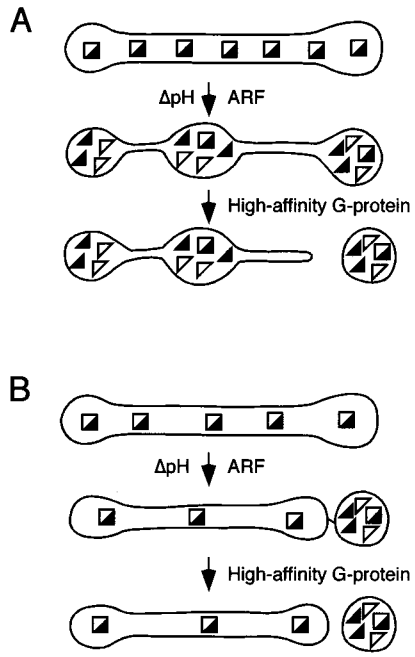

FIGURE 7: Model for the two steps reconstituted in the AtT-20 cell in vitro assay for ISG formation. The progression from the sulfation compartment (top) to the acidic POMC processing compartment (middle) to the release of the free ISG (bottom) is diagrammed for each model. Squares represent POMC and triangles represent processed POMC-derived peptides. (A) Model one: ARF regulates progranule formation during fenestration of the Golgi complex. The high-affinity GTP-binding protein then regulates scission of nascent ISGs. (B) Model two: ARF promotes budding of a nascent ISG, which remains tethered to the Golgi stack. The high affinity GTP-binding protein then promotes untethering and release of the free ISG.

Model One: Progranule Formation in Fenestrating Cisternae Followed by ISG Scission. Our biochemical data fit nicely with the elegant morphological studies by Rambourg and colleagues showing the involvement of multiple trans-Golgi cisternae during the production of ISGs (*44*). In the mucous cell of the mouse Brunner's gland, cisternae in the cis and medial portions of the Golgi are flat and contain evenly dispersed secretory material. At the start of the trans compartment, which consists of four to six cisternae in these cells, secretory material starts to condense in progranules, which appear as dilated portions of the cisternae. The cisternae become perforated at the same stage, making them appear fenestrated. In more distal cisternae, the progranules appear larger, having swelled with more secretory material, and the flattened portions appear increasingly tubular, with expanded perforations in between. At the last cisterna, the nascent ISG pinches off, leaving behind a residual network of tubular membranes (*44*). Similar processes are also seen in the pancreatic acinar cell (*21*).

We propose that the ARF-dependent step that allows the onset of prohormone processing is the formation of progranules during fenestration of the early trans-Golgi cisternae (Figure 7A). Importantly, immunoelectron microscopy with antibodies that differentiate between POMC and its various processed forms shows that processed peptides are found in dilated rims of Golgi cisternae, indicating that processing actually begins before ISGs bud from the TGN (*41*). Since POMC processing in AtT-20 cells starts in the dilated rims of Golgi cisternae in vivo, while ARF regulates the onset of POMC processing in vitro (Figure 5), we favor a model in which ARF regulates the formation of these dilated progranules during the fenestration of the trans-Golgi. Scission of these progranules would then occur at the TGN in a process regulated by a second GTP-binding protein with a higher affinity for GTPγS.

What might ARF be doing to cause this radical change in cisternal morphology? ARF could function in membrane remodeling by recruiting and activating enzymes that modify lipids on the face of the Golgi. One of ARF's well-characterized activities is the activation of PLD (*45*). Although PLD has been implicated in the production of granules (*43*, *46*), addition of bacterial PLD did not stimulate POMC processing in our system (data not shown). Another possibility is that ARF causes Golgi cisternal maturation by promoting coated vesicle budding to remove excess membrane. In this "remnant" model of ISG formation, the ISG is simply what remains of the TGN after resident Golgi proteins are recycled by coatomer-coated vesicles and endosomal proteins are removed by clathrin-coated vesicles (*47*). EM studies have found patches of both clathrin (*48*) and coatomer (*49*) on the surface of ISGs, which is consistent with involvement of these coat proteins in membrane removal from the ISG. However, removal of 85% of either clathrin or coatomer from the cytosol by immunodepletion had no effect on POMC processing in vitro (data not shown). Preliminary results from cytosol fractionation experiments also show that clathrin and coatomer are not required for POMC processing (data not shown). This is in contrast to the MDCK cell in vitro assay, in which formation of constitutive vesicles containing viral coat proteins is inhibited when coatomer is depleted from the cytosol (*50*). In our assay (Figure 5 and data not shown) and in PC12 cells (*42*), release of ISGs requires ARF but shows no coatomer dependence. The MDCK cell assay is also significantly different from our assay in other ways: vesicle release in the MDCK cell assay is stimulated by GTPγS, while our assay (Figure 4), the PC12 cell assay (*51*), and the GH_3 cell assay (*52*) are all inhibited by the GTP analogue.

Model Two: Formation of Tethered ISGs Followed by ISG Untethering. A strong alternate hypothesis to the above model is that the first stage of our assay (onset of POMC processing) corresponds to budding of ISGs from the TGN which then remain somehow tethered to the Golgi stack. In the second stage of the assay (ISG release), the nascent granules would become untethered (Figure 7B). In this model, ARF might mediate ISG budding via interaction with a coat protein. As mentioned above, this coat protein is unlikely to be clathrin or coatomer, but ARF has also been shown to recruit other adaptor complexes such as AP-3 (*55*) and AP-4 (*56*) to Golgi membranes. The role of these proteins in ISG formation remains to be established.

According to the second model, a granule tethering event regulated by an unknown GTPase protein would follow the ARF-dependent ISG budding step. Elements of the Golgi cytoskeleton might be involved in tethering of newly budded granules, and carefully regulated changes in the Golgi matrix may be required for these granules to be released (reviewed in ref *57*). Other membrane trafficking events in the Golgi are also regulated by tethering. Vesicles that mediate intra-Golgi traffic are tethered to Golgi membranes by at least three proteins: p115, giantin, and GM130. A family of

similar proteins with coiled-coil domains has been identified on the Golgi complex, any of which may be potential ISG tethering proteins (reviewed in ref *58*).

Note that to avoid confusion we have labeled the steps "onset of processing" and "granule release", avoiding the term "budding". The two proposed models place "budding" at different stages. In the first model (Figure 7A), budding is concomitant with the granule release step. In the second model (Figure 7B), budding is concomitant with the onset of processing.

Factors Determining Granule's Competency for Processing. How does ARF1-regulated budding event create a processing-competent organelle? Our finding that acidification of the donor membrane can obviate the requirement for budding (Figure 3) suggests that a change in lumenal pH during budding is most likely responsible for acquisition of processing competency. This interpretation is consistent with our finding that inihibitors of the V-ATPase (BafA1 and NEM) also inhibited POMC processing (Figures 1 and 2). Recently, we have directly measured the pH of secretory compartments in live AtT-20 cells (*13*). The trans-Golgi of these cells was found to maintain an average pH of 6.2, while mature secretory granules have an average pH of 5.5. This is in excellent agreement with the pH dependency of POMC processing observed in vitro (Figure 3). Furthermore, we have found that secretory granules achieve a more acidic pH than the trans-Golgi due to a smaller proton leak rate. We propose that an essential step in gaining processing competency is sorting of proton pumps and leaks during ARF-mediated budding.

Ionic milieu also plays a key role in Furin activation: exposure of membranes containing an ER-localized Furin to ionic (acidic and calcium-containing) environment of the TGN can fully activate this otherwise inactive enzyme (*7*). By contrast, processing of secretogranin II by SPC2 cannot be activated by acidifying the TGN to pH mimicking ISGs (*40*); in this system, factors other than ionic milieu must also play a role to effect processing. Contradictory data also exist in the literature regarding the requirement for acidic pH in POMC processing. In one study, dissipation of granule pH gradient with weak bases did not interfere with POMC processing in AtT-20 cells (*59*). In another study, the degree of POMC processing in individual granule was found to be positively correlated with its acidity (*39*). The origin of these discrepancies remains unclear but could be due to ineffective neutralization of granule pH by different drug treatment of intact cells.

Presently we do not know the identity of the GTP-binding protein involved in ISG release. Pretreatment of AtT-20 cells with the heterotrimeric G-protein modulators cholera toxin or pertussis toxin, which affected granule formation from PC12 cells (*60*), had no effect on either onset of processing or ISG release (data not shown). We also investigated the role of dynamin II, which have been implicated in protein export from the TGN via both the constititutive (*23*) and regulated secretory pathways (*61*) (although a contradictory view has also been presented, see ref *62*). Neither POMC processing nor ISG release was inhibited by two dynamin II inhibitory antibodies (MC63 and Dyn2) (data not shown). Finally, we investigated the role of the Rab family of GTPases that have also been implicated in vesicle formation (*63*). Rab3 could be involved in ISG formation at the TGN, as it is specifically expressed in professional secretory cells and localizes to secretory granules (*64*). Addition of purified Rab GDI to the in vitro reaction, which removed over 90% of Rab3 from the donor membrane fraction, had no effect on granule release and only slightly inhibited POMC processing (data not shown).

In sum, much remains to be learned about the process of secretory granule production from the trans-Golgi. The two-step assay that we describe here should provide a powerful system to dissect the key components regulating prohormone processing and secretory granule biogenesis.

REFERENCES

1. Steiner, D. F. (1998) *Curr. Opin. Chem. Biol. 2*, 31−9.
2. Seidah, N. G., and Chrétien, M. (1999) *Brain Res. 848*, 45−62.
3. Bergeron, F., Leduc, R., and Day, R. (2000) *J. Mol. Endocrinol. 24*, 1−22.
4. O'Rahilly, S., Gray, H., Humphreys, P. J., Krook, A., Polonsky, K. S., White, A., Gibson, S., Taylor, K., and Carr, C. (1995) *New Engl. J. Med. 333*, 1386−1390.
5. Jackson, R. S., Creemers, J. W. M., Ohagi, S., and Raffin-Sanson, M. L. (1997) *Nat. Genet. 16*, 303−306.
6. Hubbard, F. C., Goodrow, T. L., Liu, S. C., Brilliant, M. H., Basset, P., Mains, R. E., and Klein-Szanto, A. J. (1997) *Cancer Res. 57*, 5226−5231.
7. Anderson, E. D., Vanslyke, J. K., Thulin, C. D., Jean, F., and Thomas, G. (1997) *EMBO J. 16*, 1508−1518.
8. Martens, G. J., Braks, J. A., Eib, D. W., Zhou, Y., and Lindberg, I. (1994) *Proc. Natl. Acad. Sci. U.S.A. 91*, 5784−5787.
9. Qian, Y., Devi, L. A., Mzhavia, N., Munzer, S., Seidah, N. G., and Fricker, L. D. (2000) *J. Biol. Chem. 275*, 23596−23601.
10. Cameron, A., Fortenberry, Y., and Lindberg, I. (2000) *Febs Lett. 473*, 135−138.
11. Schmidt, W. K., and Moore, H.-P. H. (1995) *Mol. Biol. Cell 6*, 1271−1285.
12. Schapiro, F. B., and Grinstein, S. (2000) *J. Biol. Chem. 275*, 21025−21032.
13. Wu, M., Grabe, M., Adams, S., Tsien, R. Y., Moore, H. P. H., and Machen, T. E. (2001) *J. Biol. Chem. 276*, 33027−33035.
14. Xu, H., and Shields, D. (1994) *J. Biol. Chem. 269*, 22875−22881.
15. Tooze, S. A., and Huttner, W. B. (1990) *Cell 60*, 837−847.
16. Mains, R. E., and Eipper, B. A. (1978) *J. Biol. Chem. 253*, 651−655.
17. Benjannet, S., Rondeau, N., Day, R., Chretien, M., and Seidah, N. (1991) *Proc. Natl. Acad. Sci. 88*, 3564−3568.
18. Thomas, L., Leduc, R., Smeekens, S. P., Steiner, D. F., and Thomas, G. (1991) *Proc. Natl. Acad. Sci. U.S.A. 88*, 5297−5301.
19. Zhou, A., Bloomquist, B. T., and Mains, R. E. (1993) *J. Biol. Chem. 268*, 1763−1769.
20. Fernandez, C., Haugwitz, M., Eaton, B., and Moore, H. P. H. (1997) *Mol. Biol. Cell 8*, 2171−2185.
21. Rambourg, A., Clermont, Y., and Hermo, L. (1988) *Am. J. Anat. 183*, 187−199.
22. Tsien, R., and Pozzan, T. (1989) *Methods Enzymol. 172*, 230−262.
23. Jones, S. M., Howell, K. E., Henley, J. R., Cao, J., and McNiven, M. A. (1998) *Science 279*, 573−577.
24. Shapiro, A. D., and Pfeffer, S. R. (1995) *J. Biol. Chem. 270*, 11085−11090.
25. Randazzo, P. A., Weiss, O., and Kahn, R. A. (1992) *Methods Enzymol. 219*, 362−369.
26. Chen, Y. G., and Shields, D. (1996) *J. Biol. Chem. 271*, 5297−300.
27. Miller, S. G., and Moore, H.-P. H. (1991) *J. Cell Biol. 112*, 39−54.

28. Morinaga, N., Adamik, R., Moss, J., and Vaughan, M. (1999) *J. Biol. Chem. 274*, 17417−17423.
29. Mansour, S. J., Skaug, J., Zhao, X. H., Giordano, J., Scherer, S. W., and Melançon, P. (1999) *Proc. Natl. Acad. Sci. 96*, 7968−7973.
30. Mellman, I., Fuchs, R., and Helenius, A. (1986) *Annu. Rev. Biochem. 55*, 663−700.
31. Bowman, E. J., Siebers, A., and Altendorf, K. (1988) *Proc. Natl. Acad. Sci. U.S.A. 85*, 7972−7976.
32. Jean, F., Basak, A., Rondeau, N., Benjannet, S., Hendy, G. N., Seidah, N. G., Chretien, M., and Lazure, C. (1993) *Biochem. J. 292*, 891−900.
33. Rufaut, N. W., Brennan, S. O., Hakes, D. J., Dixon, J. E., and Birch, N. P. (1993) *J. Biol. Chem. 268*, 20291−20298.
34. Zhou, Y., and Lindberg, I. (1993) *J. Biol. Chem. 268*, 5615−5623.
35. Schwartz, N. B., Galligani, L., Ho, P.-L., and Dorfman, A. (1974) *Proc. Natl. Acad. Sci. U.S.A. 71*, 4047−4051.
36. Burgess, T. L., and Kelly, R. B. (1984) *J. Cell Biol. 99*, 2223−2230.
37. Farinas, J., and Verkman, A. S. (1999) *J. Biol. Chem. 274*, 7603−7606.
38. Tooze, J., Hollinshead, M., Frank, R., and Burke, B. (1987) *J. Cell Biol. 105*, 155−162.
39. Tanaka, S., Yora, T., Nakayama, K., Inoue, K., and Kurosumu, K. (1997) *J. Histochem., Cytochem. 45*, 425−436.
40. Urbé, S., Dittié, A. S., and Tooze, S. A. (1997) *Biochem. J. 321*, 65−74.
41. Schnabel, E., Mains, R. E., and Farquhar, M. G. (1989) *Mol. Endocrinol. 3*, 1223−1235.
42. Barr, F. A., and Huttner, W. B. (1996) *FEBS Lett. 384*, 65−70.
43. Chen, Y. G., Sidddhanta, A., Austin, C. D., Hammond, S. M., Sung, T. C., Frohman, M. A., Morris, A. J., and Shields, D. (1997) *J. Cell Biol. 138*, 495−504.
44. Rambourg, A., Clermont, Y., Hermo, L., and Segrétain, D. (1987) *Am. J. Anat. 179*, 95−107.
45. Brown, H. A., Gutowski, S., Moomaw, C. R., Slaughter, C., and Sternweis, P. C. (1993) *Cell 75*, 1137−1144.
46. Tüscher, O., Lorra, C., Bouma, B., Wirtz, K. W. A., and Huttner, W. B. (1997) *FEBS Lett. 419*, 271−275.
47. Glick, B. S., and Malhotra, V. (1998) *Cell 95*, 883−889.
48. Orci, L., Ravazzola, M., Amherdt, M., Louvard, D., and Perrelet, A. (1985) *Proc. Natl. Acad. Sci. U.S.A. 82*, 5385−5389.
49. Martinez-Menarguez, J. A., Geuze, H. J., Slot, J. W., and Klumperman, J. (1999) *Cell 98*, 81−90.
50. Simon, J.-P., Shen, T.-H., Ivanov, I. E., Gravotta, D., Morimoto, T., Adesnik, M., and Sabatini, D. D. (1998) *Proc. Natl. Acad. Sci. U.S.A. 95*, 1073−1078.
51. Tooze, S. A., Weiss, U., and Huttner, W. B. (1990) *Nature 347*, 207−208.
52. Xu, H., and Shields, D. (1993) *J. Biol. Chem. 122*, 1169−1184.
53. Faundez, V., Horng, J. T., and Kelly, R. B. (1997) *J. Cell Biol. 138*, 505−515.
54. Zhu, Y., Traub, L. M., and Kornfeld, S. (1998) *Mol. Biol. Cell 9*, 1323−1337.
55. Ooi, C. E., Dell'Angelica, E. C., and Bonifacino, J. S. (1998) *J. Cell Biol. 142*, 391−402.
56. Dell'Angelica, E. C., Mullins, C., and Bonifacino, J. S. (1999) *J. Biol. Chem. 274*, 7278−7285.
57. Lorra, C., and Huttner, W. B. (1999) *Nat. Cell Biol. 1*, E113−E115.
58. Waters, M. G., and Pfeffer, S. R. (1999) *Curr. Opin. Cell Biol. 11*, 453−459.
59. Mains, R. E., and May, V. (1988) *J. Biol. Chem. 263*, 7887−7894.
60. Leyte, A., Barr, F. A., Kehlenbach, R. H., and Huttner, W. B. (1992) *EMBO J. 11*, 4795−4804.
61. Yang, Z. Y., Li, H., Chai, Z. L., Fullerton, M. J., Cao, Y., Toh, B. H., Funder, J. W., and Liu, J. P. (2001) *J. Biol. Chem. 276*, 4251−4260.
62. Altschuler, Y., Barbas, S. M., Terlecky, L. J., Tang, K., Hardy, S., Mostov, K. E., and Schmid, S. L. (1998) *J. Cell Biol. 143*, 1871−81.
63. Allan, B. B., Moyer, B. D., and Balch, W. E. (2000) *Science 289*, 444−448.
64. Darchen, F., Zahraoui, A., Hammel, F., Monteils, M. P., Tavitian, A., and Scherman, D. (1990) *Proc. Natl. Acad. Sci. 87*, 5692−5696.

BI0112762